Supplementary Information for

Coprinopsis cinerea dioxygenase is an oxygenase forming 10(*S*)-hydroperoxide of linoleic acid, essential for formation of mushroom alcohol, 1-octen-3-ol

Takuya Teshima, Risa Funai, Takehito Nakazawa, Junya Ito, Toshihiko Utsumi, Pattana Kakumyan, Hiromi Mukai, Toyoshi Yoshiga, Ryutaro Murakami, Kiyotaka Nakagawa, Yoichi Honda, Kenji Matsui*

*Kenji Matsui
Email: matsui@yamaguchi-u.ac.jp

This PDF file includes:
Figures S1 to S15
Tables S1 to S4

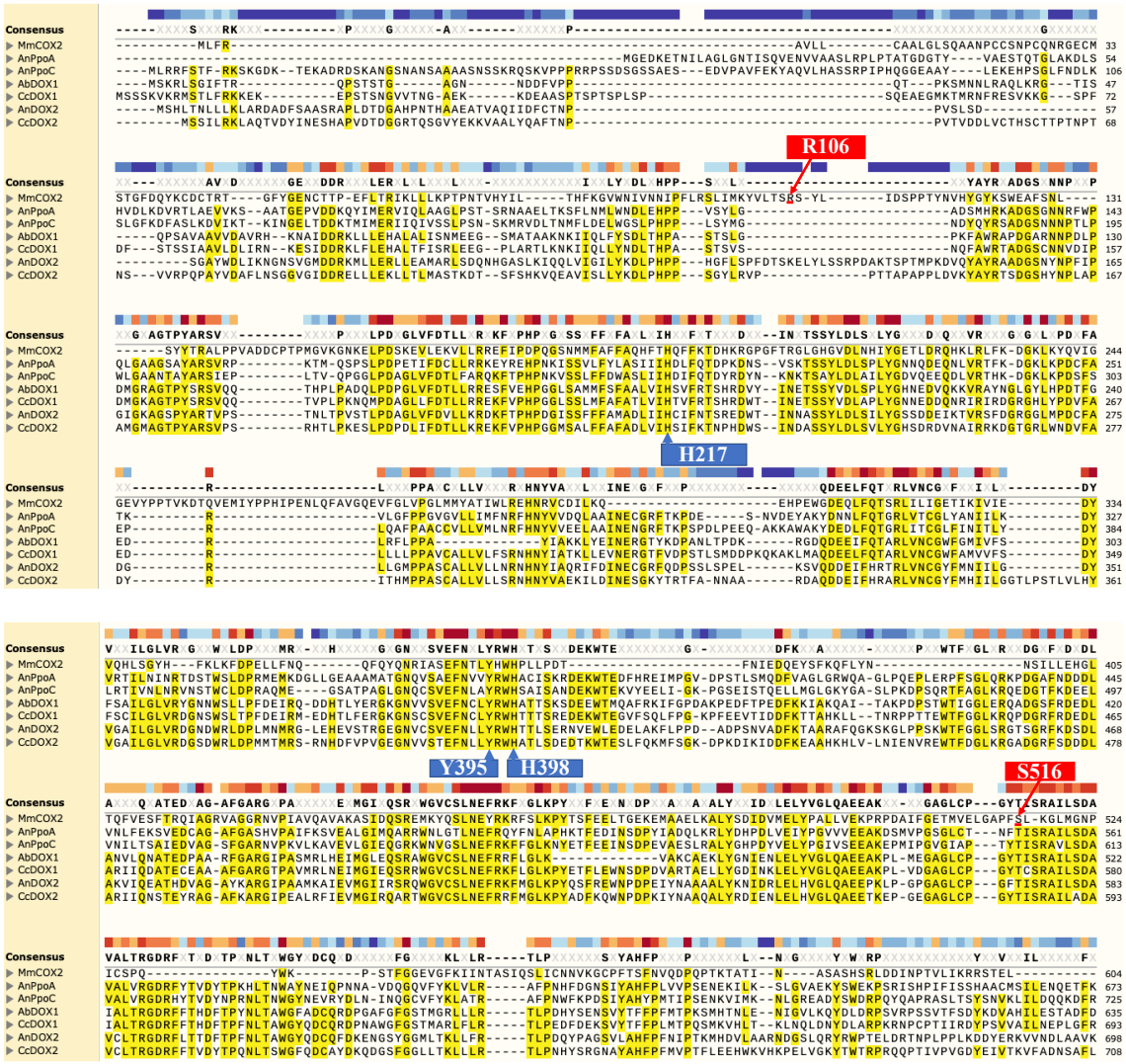

Fig. S1. Alignment of the N-terminal DOX domains of *A. nidulans* AnPpoA (GenBank; AAR88626.1), AnPpoC (AAT36614.1), *C. cinerea* CcDOX1 (EAU90460.2), CcDOX2 (EAU86789.2), *Agaricus bisporus* AbDOX1 (EKV46570.1), AbDOX2 (EKV43127.1), and mouse (*Mus musculus*) MmCOX2 (Q05769.1). The amino acid residues described in the text are indicated by colored arrows with numbering based on the CcDOX1 (blue background) and MmCOX2 (red background) sequences, respectively.

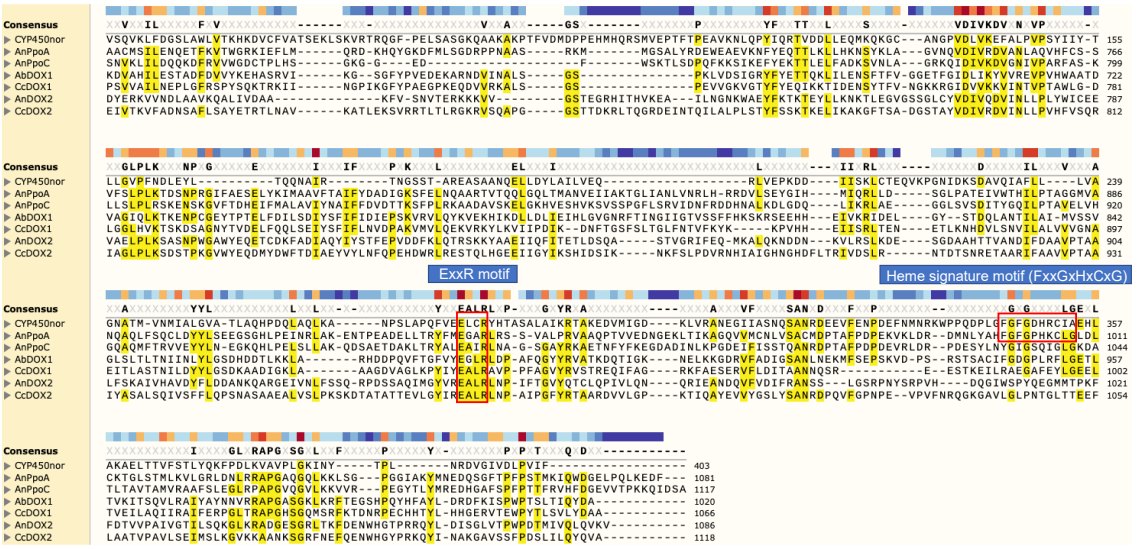

Fig. S2. Alignment of the C-terminal cytochrome P450 domains of AnPpoA, AnPpoC, CcDOX1, CcDOX2, AbDOX1, AbDOX2, and *Fusarium oxysporum* CYP450nor (P23295.2). The ExxR motif widely conserved in P450 enzymes and the heme signature motif (FxxGxHxCxG) essential for P450 activities are highlighted.

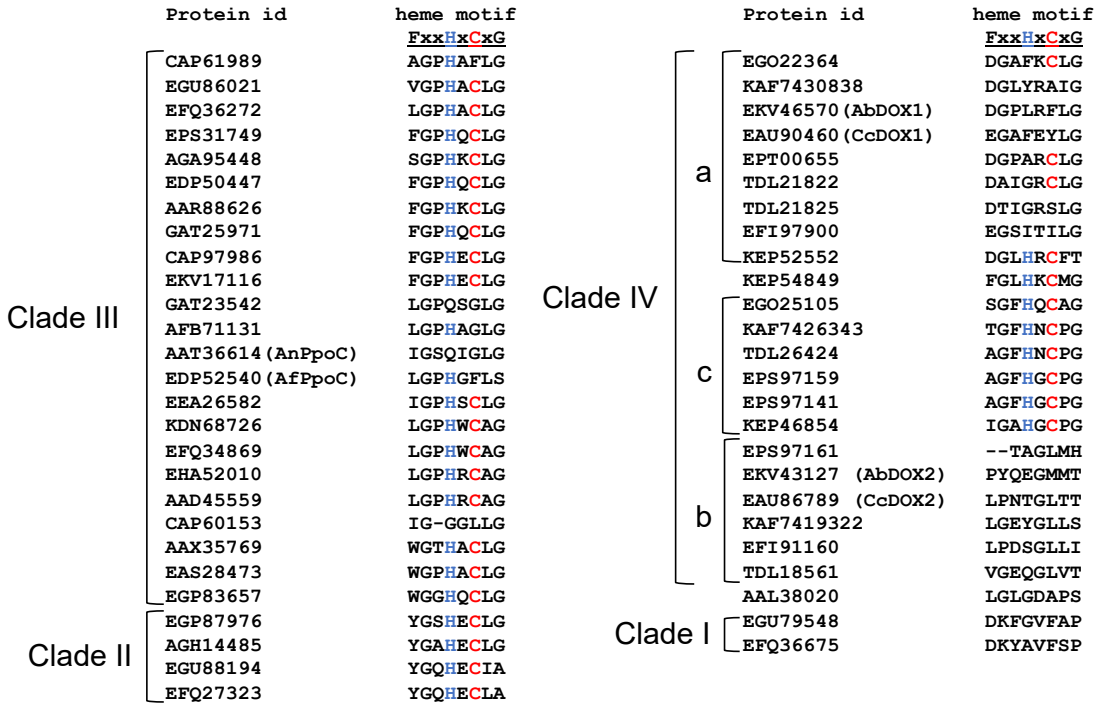

Fig. S3. Alignment of the heme signature motif (FxxGxHxCxG) from the protein sequences used for the construction of the phylogenetic tree shown in Fig. 3B.

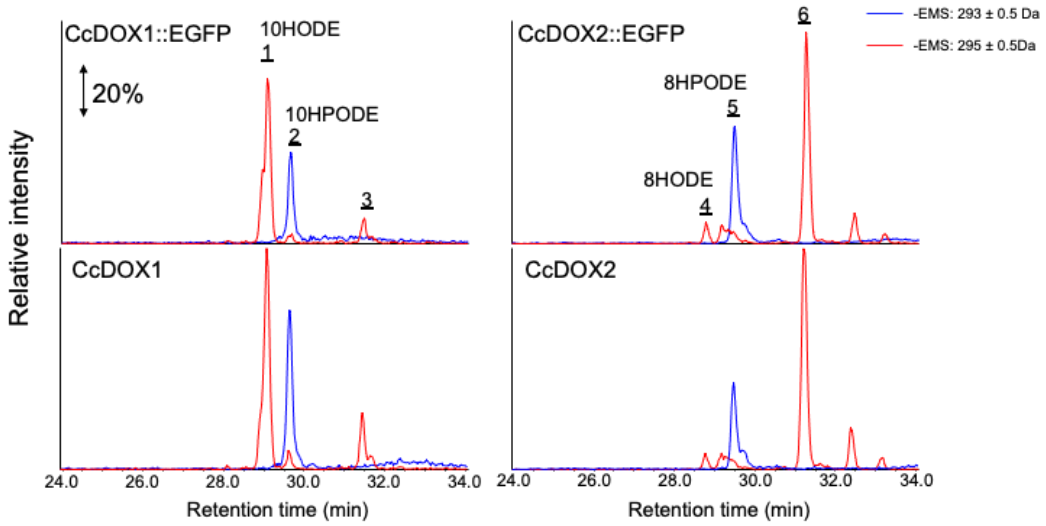

Fig. S4. Products formed by insect cell-expressed recombinant CcDOX1 and CcDOX2 with/without EGFP. The crude lysate of the insect cells expressing CcDOX1, CcDOX1 fused with EGFP (CcDOX1::EGFP), CcDOX2, and CcDOX2 fused with EGFP (CcDOX2::EGFP) had linoleic acid added to them, and the products were analyzed in the negative enhanced mass spectrum mode of LC-MS/MS. Chromatograms of extracted ions of *m/z* 293.0 ± 0.5 corresponding to linoleic acid hydroperoxide $[M\text{-}H_3O^+]^-$ and *m/z* 295.0 ± 0.5 corresponding to linoleic acid hydroxide $[M\text{-}H^+]^-$ are shown in blue and red, respectively. Peak 1 and 2 were tentatively assigned as 10HODE and 10HPODE, respectively. Peak 4 and 5 were tentatively assigned as 8HODE and 8HPODE, respectively. The conversion of hydroperoxide into hydroxide was likely catalyzed by an unknown enzyme in the insect cells. Peak 3 and 6 were likely derived from oleic acid endogenous to insect cells.

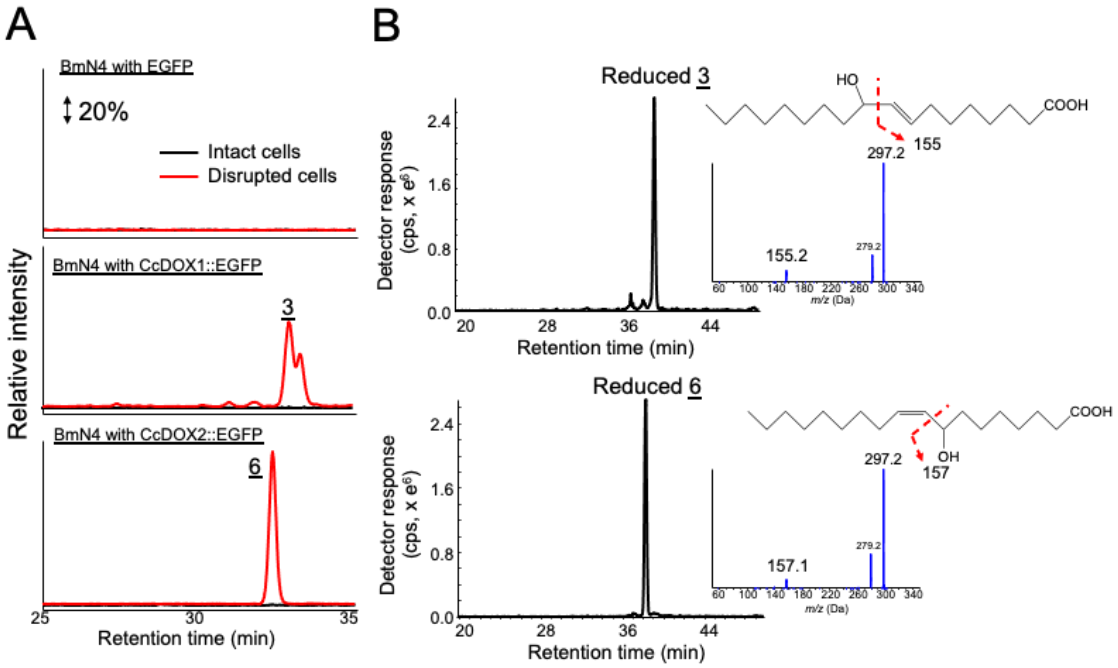

Fig. S5. Products formed by the insect cells (BmN4) expressing EGFP, CcDOX1::EGFP, or CcDOX2::EGFP. (A) The intact cells (black line) or the cells after disruption with a sonicator (red line) were extracted with ethanol for LC-MS/MS analysis in the negative enhanced mass spectrum. Chromatograms of extracted ions of *m/z* 295.0 ± 0.5 corresponding to oleic acid hydroperoxide $[C_{18}H_{34}O_4\text{-}H_3O^+]^-$ are shown. (B) The products formed in the disrupted insect cells containing recombinant CcDOX1 (upper) and CcDOX2 (lower) were reduced with triphenylphosphine, and served for LC-MS/MS analysis in the enhanced product ion mode with *m/z* 297.2 $[C_{18}H_{34}O_3\text{-}H^+]^-$ as the parent ion. Based on the fragment profiles, reduced 3 and reduced 6 were tentatively assigned as 10- and 8-hydroxide of oleic acid, respectively.

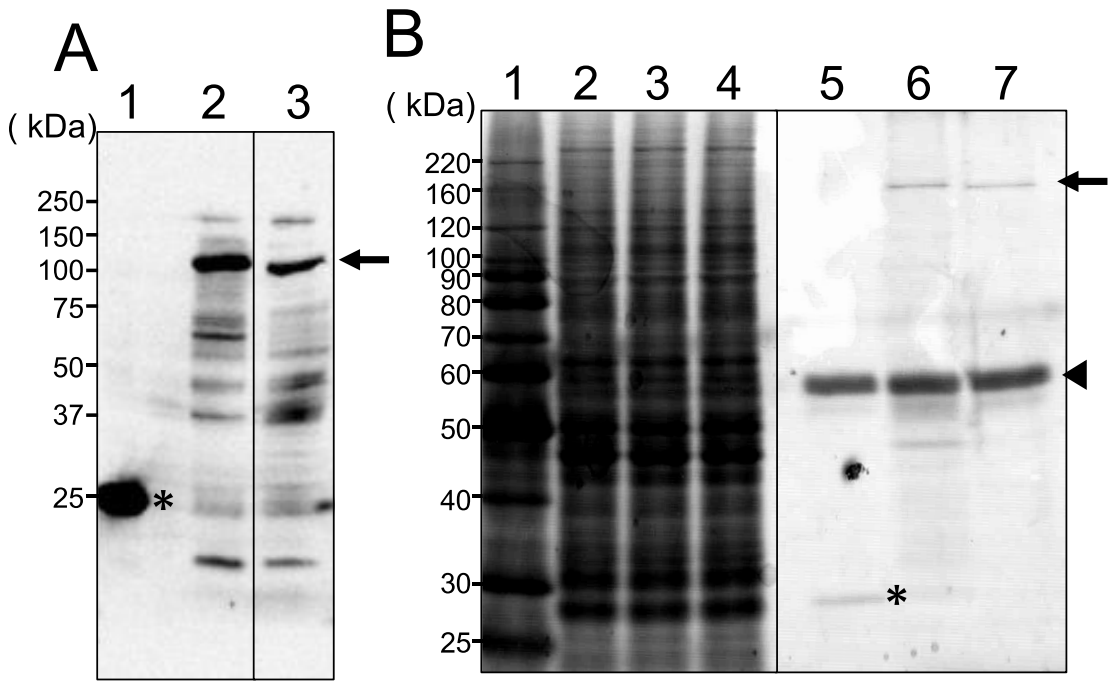

Fig. S6. Expression of recombinant CcDOX1 and CcDOX2 in BmN4 cells. (A) Immunoblot analysis with crude extract expressing EGFP (shown with an asterisk in lane 1, ca. 27 kDa), CcDOX1::EGFP fusion protein (lane 2), and CcDOX2::EGFP fusion protein (lane 3). The arrow indicates the protein bands corresponding to the fusion proteins. (B) CBB-staining of the crude extract expressing EGFP (lane 2), CcDOX1::EGFP fusion protein (lane 3), CcDOX2::EGFP fusion protein (lane 4), immunoprecipitated fraction of the lysate expressing EGFP only (lane 5), immune-purified CcDOX1::EGFP fusion protein (lane 6), and immune-purified CcDOX2::EGFP fusion protein (lane 7). The positions of the fusion protein (147 kDa) and the heavy chain of rabbit immunoglobulin (ca. 50 kDa) used for purification are shown with an arrow and a triangle, respectively. The asterisk in the lane 5 indicates the protein bands corresponding to EGFP. Lane 1: molecular weight marker.

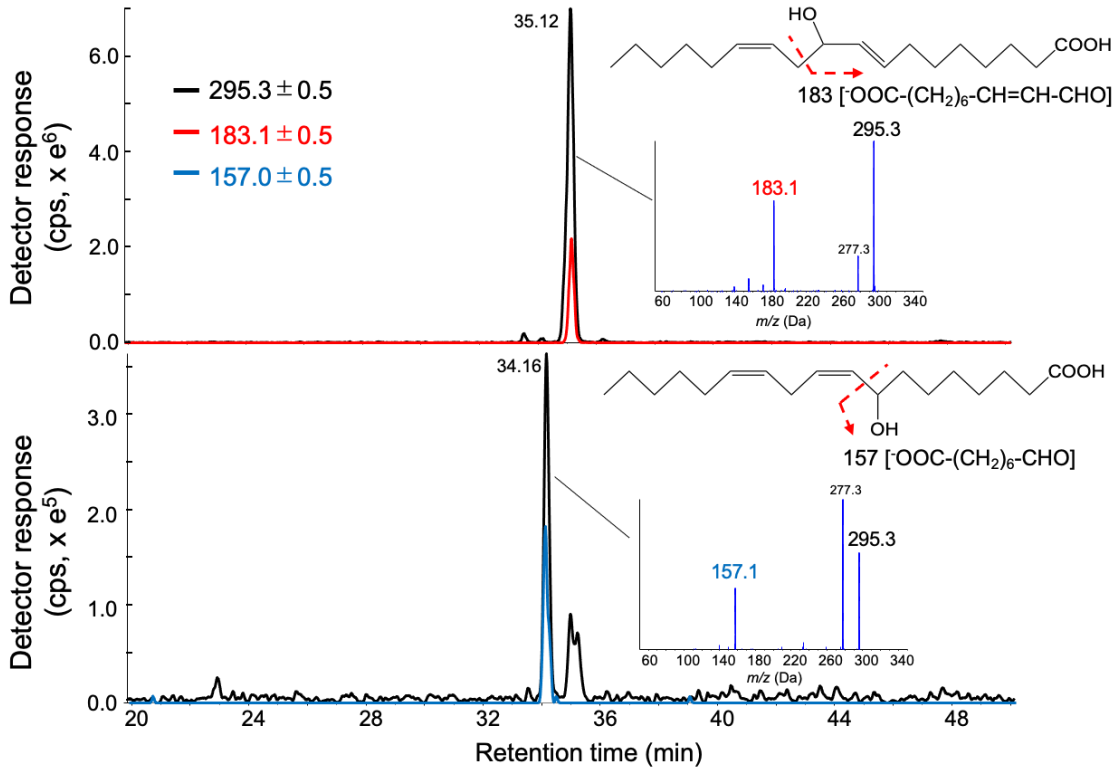

Fig. S7. Chromatograms with the products formed by immuno-purified recombinant CcDOX1::EGFP (upper) and immuno-purified recombinant CcDOX2::EGFP (lower) from linoleic acid. The chromatograms were obtained with LC-MS/MS in the negative enhanced product ion mode. The products were reduced with triphenylphosphine before analysis. The negative ion of *m/z* 295.30 corresponding to the hydroxides of linoleic acid $[M\text{-}H^+]^-$ was chosen as the parent ion. The black line is shown with the parent ion, and the red and blue lines are drawn with *m/z* 183.1 and *m/z* 157.1, corresponding the fragment ions diagnostic to 10- and 8-hydroxides of linoleic acid. The mass spectrum for each main peak is shown in the inset with expected fragmentation pattern.

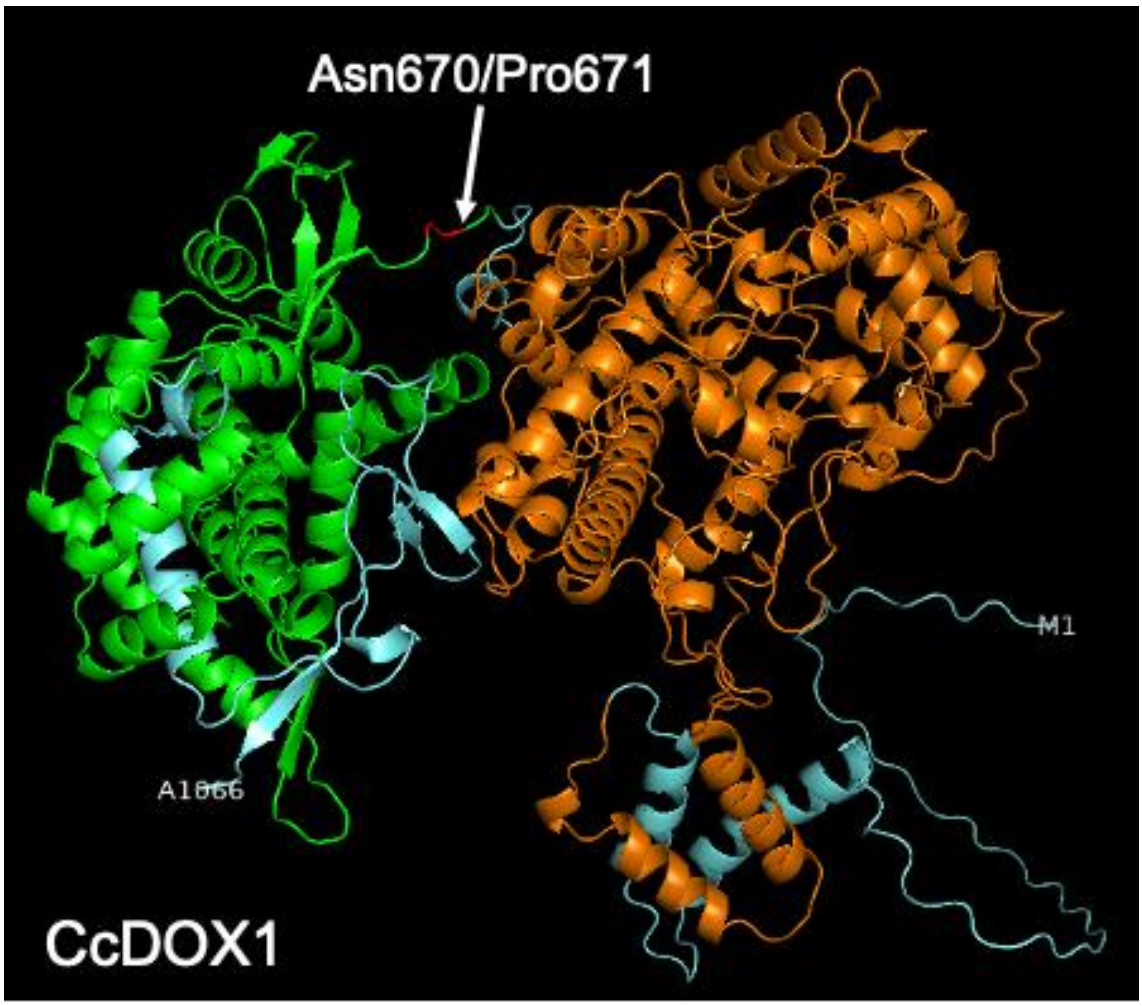

Fig. S8. The 3D structure of CcDOX1 predicted with AlphaFold2. The N-terminal DOX domains are shown in orange, the C-terminal P450-related domains in green, and the other regions in cyan. The predicted junction between the DOX domains and the P450-related domains are shown with a white arrow.

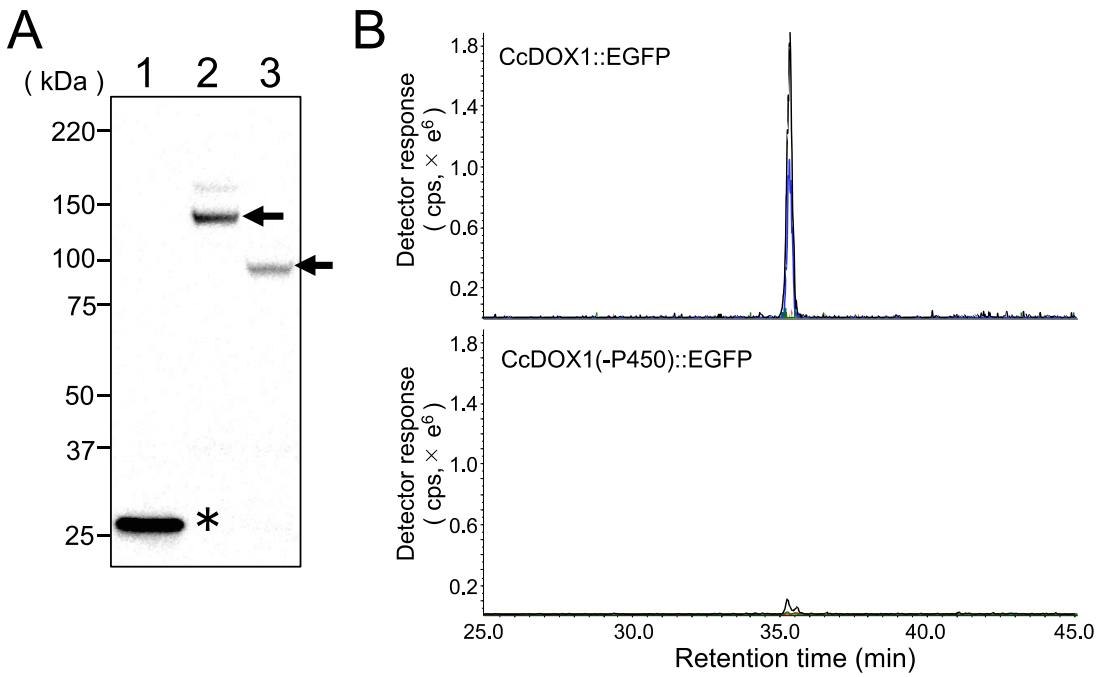

Fig. S9. Deletion of the C-terminal P450-related domain from CcDOX1 resulted in loss of activity. (A) Immunoblot analysis with the immune-purified EGFP (shown with an asterisk in lane 1, ca. 27 kDa), CcDOX1::EGFP fusion protein (lane 2), and CcDOX1 without P450-related domain::EGFP fusion protein (lane 3). The arrow indicates the protein bands corresponding to the fusion proteins. (B) Chromatograms with the products formed by immuno-purified recombinant CcDOX1::EGFP (upper) and immuno-purified recombinant CcDOX1 without P450-related domain (CcDOX1(-P450)::EGFP (lower) from linoleic acid. The chromatograms were obtained with LC-MS/MS in the negative enhanced product ion mode. The products were reduced with triphenylphosphine before analysis. The negative ion of *m/z* 295.30 corresponding to the hydroxides of linoleic acid $[M\text{-}H^+]^-$ was chosen as the parent ion. The black line is shown with the parent ion, and the blue, red, and green lines are drawn with *m/z* 183.1, *m/z* 171.1, and *m/z* 195.1, corresponding the fragment ions diagnostic to 10-, 9-, and 13-hydroxides of linoleic acid.

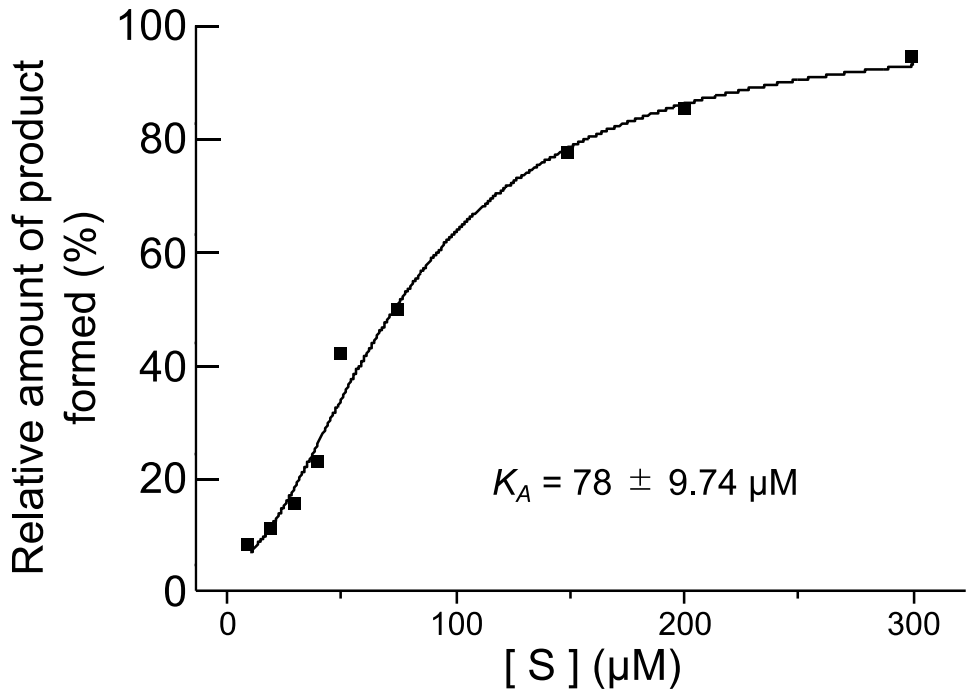

Fig. S10. [S]-v plot of recombinant CcDOX1 with linoleic acid. The relative amount of product obtained with LC-MS/MS with negative enhanced MS mode was fitted to the Hill equation (n = 1.86 ± 0.27) with correlation coefficient (r^2) of 0.9899 by using Origin software. The value obtained with 1000 μM was set at 100%. K_A is the ligand concentration producing half occupation.

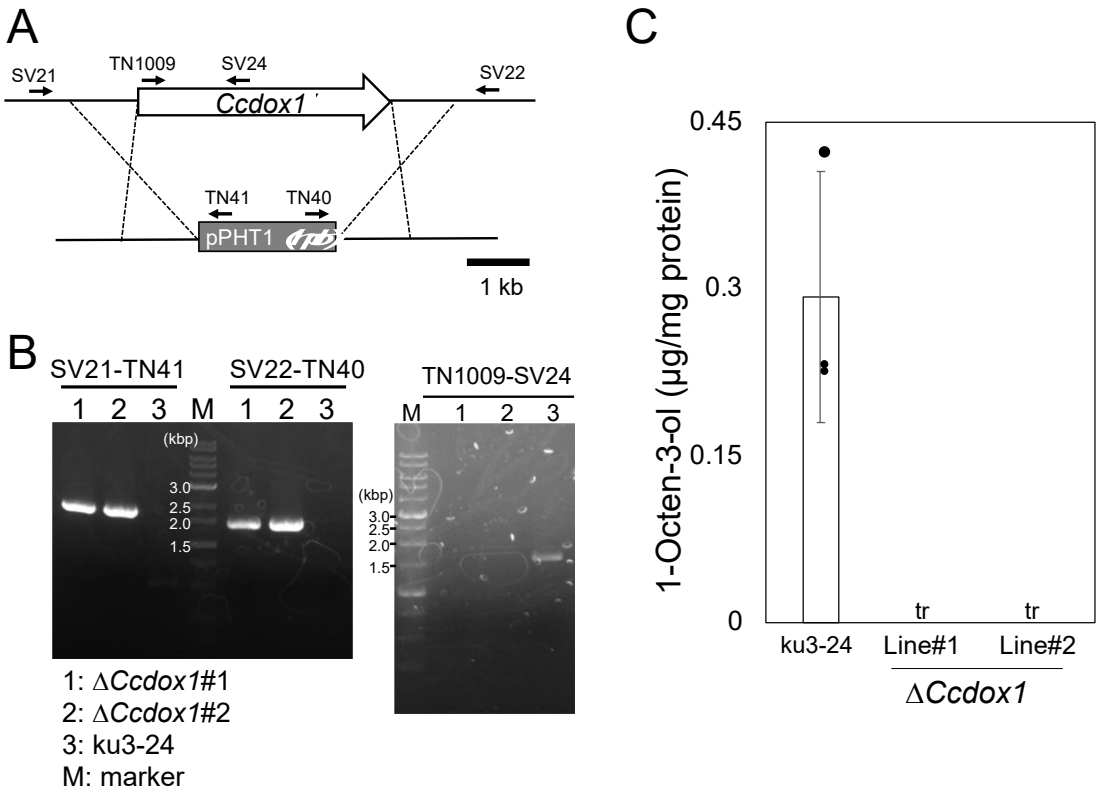

Fig. S11. Disruption of *Ccdox1* gene. (A) Schematic diagram of gene disruption through homologous recombination. Primers used for the PCR reactions are shown. (B) PCR analysis to confirm the deletion of *Ccdox1* using genomic DNA as template. The primer sets used in this study are shown in Table S4. (C) Amount of 1-octen-3-ol formed by the ku3-24 and two Δ*Ccdox1* strains.

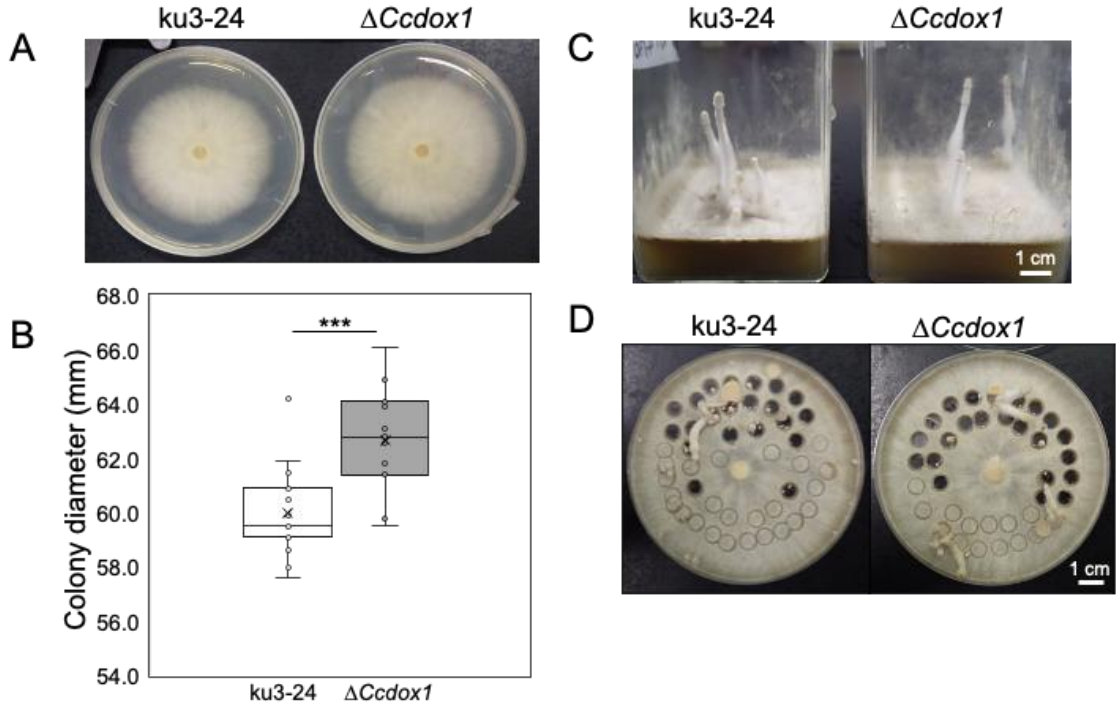

Fig. S12. Growth phenotypes of the wildtype and Δ*Ccdox1* mycelia grown on YMG medium. (A) Colonies formed on the 5th day after the onset of culture on YMG medium. (B) Diameters of mycelial colonies measured on the 5th day are presented in the respective boxplots. Statistically significant differences between ku3-24 and Δ*Ccdox1* were determined by Student's t-test. ***P < 0.001; *n* = 15. (C) Fruiting bodies formed on the 32nd day after the onset of culture on YMG medium. (D) Fruiting bodies formed on the 11th day after cutting the mycelia grown for 9 days.

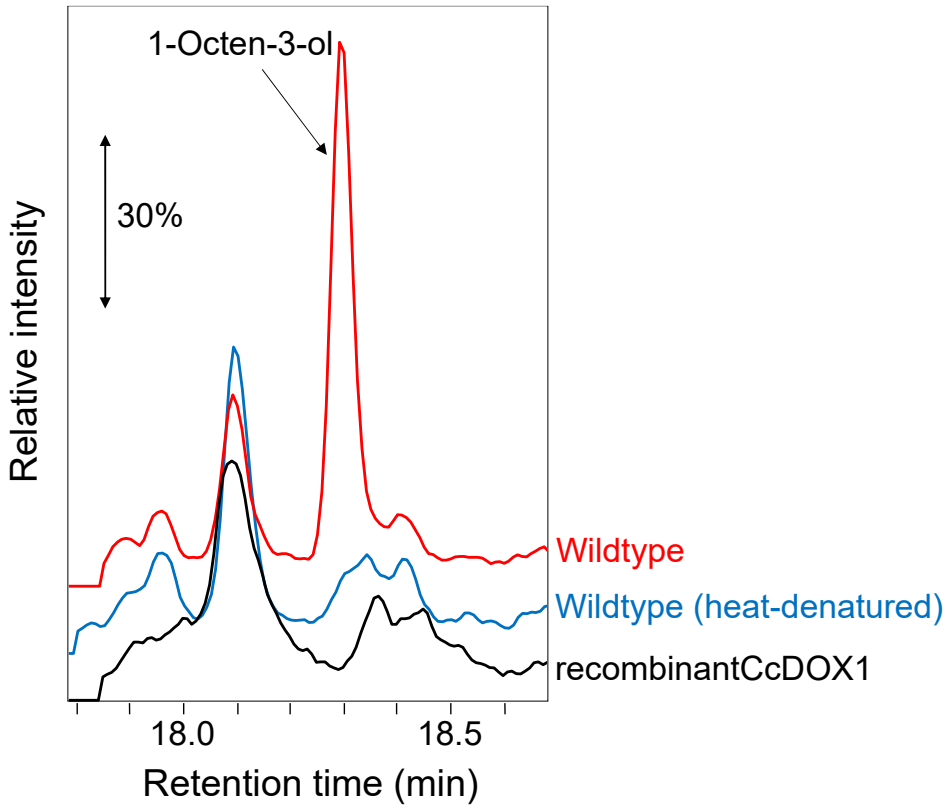

Fig. S13. The formation of 1-octen-3-ol from 10(*S*)HPODE with microsome fraction prepared with the mycelia of *C. cinerea* (red trace) and with immune-purified CcDOX1 expressed in insect cells (black). As it was anticipated that 10(*S*)HPODE spontaneously degraded to yield 1-octen-3-ol, the microsomal fraction was heat-denatured and used as the enzyme source (blue). The molecular ion chromatogram with the fragment ion of *m/z* 72 that is specific to 1-octen-3-ol is shown.

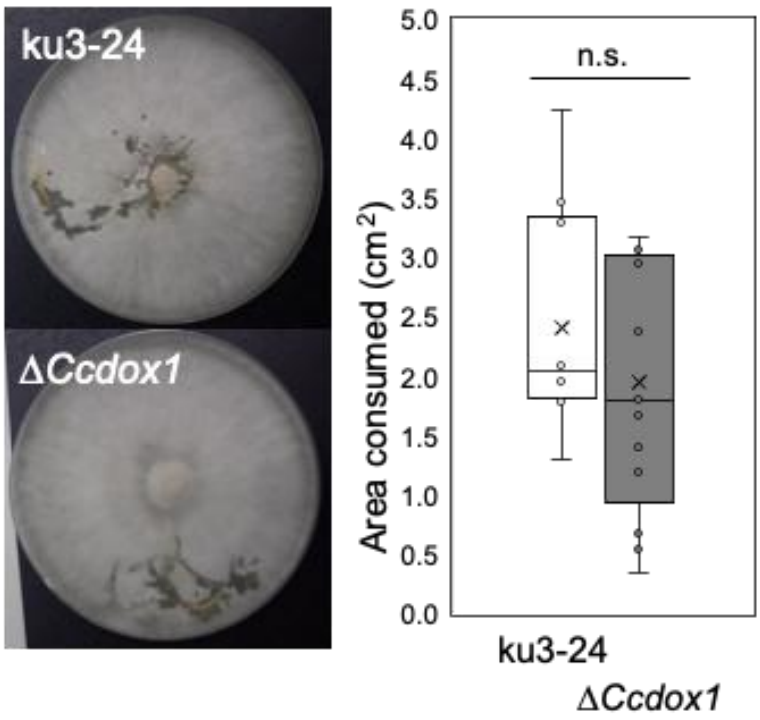

Fig. S14. Feeding behavior (left) of *Neoempheria dilatata* on Δ*Ccdox1* and its parent strain (ku3-24) on YMG medium. The area consumed by the larvae (right) after 24 h was measured with ImageJ. There was no statistically significant difference between the two genotypes (n =10, Student's t-test).

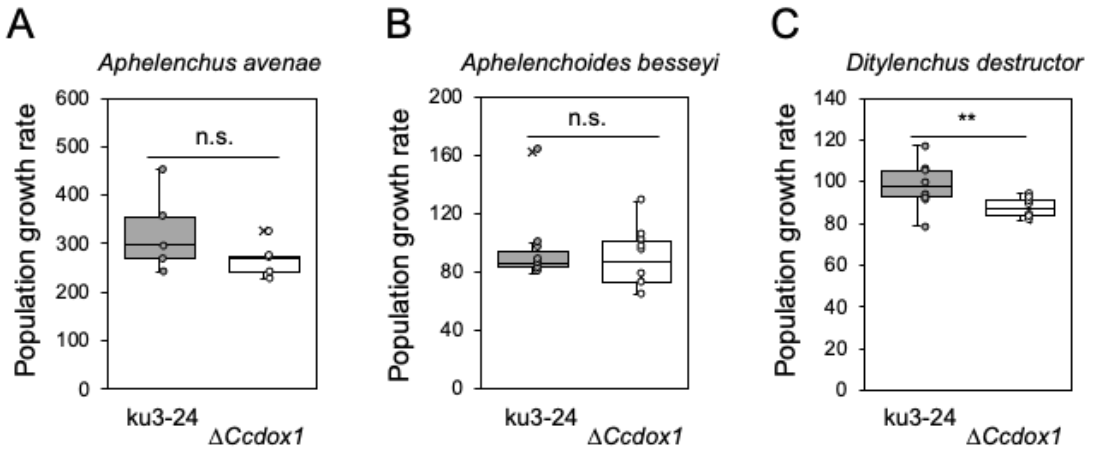

Fig. S15. Nematode propagation on *Coprinopsis cinerea* Δ*Ccdox1* and its parent strain ku3-24. (A) *Aphelenchus avenae*, (B) *Aphelenchoides besseyi*, and (C) *Ditylenchus destructor*. Data from 5 (*A. avenae*) and 10 (*A. besseyi* and *D. destructor*) independent experiments are presented in the respective boxplots. Statistically significant differences between ku3-24 and Δ*Ccdox1* were determined by Student's *t*-test. $^{**}P < 0.01$.

Table S1. Proteins used to construct the phylogenetic tree shown in Fig. 3B.

Scientific name	Scientific classification	GenBank	RefSeq / protein_id	CDS / locus_tag	Products/Enzyme name
Nostoc punctiforme PCC 73102	Cyanobacteria	ACC83776.1	WP_012411722.1	NPUN_RS27670	10(S)-HPODE
Podospora anserina	Ascomycota	CAP61989.1	XP_001904211.1	PODANS_5_1240 (PaCOX2)	10-HODE/1-octen-3ol
Fusarium oxysporum	Ascomycota	EGU86021.1		FOXB_03425	10R-DOX-EAS
Colletotrichum graminicola	Ascomycota	EFQ36272.1	XP_008100292.1	GLRG_11417	7,8-LDS/8,11-dihydroxylinoleic acid
Penicillium oxalicum 114-2	Ascomycota	EPS31749.1		PDE_06706	7S,8S-DiHODE
Aspergillus terreus	Ascomycota	AGA95448.1	XP_001213170.1	ATEG_03992	5,8-LDS
Aspergillus fumigatus A1163	Ascomycota	EDP50447.1		AFUB_067850	5,8-LDS/PpoA
Aspergillus nidulans	Ascomycota	AAR88626.1			8-HODE(/5S,8R)-DiHODE/PpoA
Penicillium chrysogenum	Ascomycota	CAP97986.1	XP_002564723.1	PCH_Pc22g06980	8 R ,11 S -DiHODE/8-HODE
Penicillium digitatum	Ascomycota	EKV17116.1	XP_014535919.1	PDIP_33150	8-HODE
Aspergillus lunchuensis	Ascomycota	GAT23542.1		RIB2604_01706810	PpoC (involved in 1-octen-3-ol formation)
Aspergillus lunchuensis	Ascomycota	GAT25971.1		RIB2604_02005510	PpoA
Aspergillus terreus	Ascomycota	AFB71131.1		ATEG_04755	10(R)-DOX
Aspergillus nidulans	Ascomycota	AAT36614.1			10-HPODE/PpoC
Aspergillus fumigatus A1163	Ascomycota	EDP52540.1		AFUB_037060	(10R)-dioxygenases/PpoC
Penicillium marneffei	Ascomycota	EEA26582.1	XP_002147129.1	PMAA_076430	10(R)-DOX/PpoC
Colletotrichum sublineola	Ascomycota	KDN68726.1		CSUB01_04826	7,8-LDS/8,11-dihydroxylinoleic acid
Colletotrichum graminicola	Ascomycota	EFQ34869.1	XP_008098889.1	GLRG_10013	7,8-LDS/8,11-dihydroxylinoleic acid
Magnaporthe oryzae	Ascomycota	EHA52010.1	XP_003711817.1	MGG_13239	7,8-LDS
Gaeumannomyces graminis	Ascomycota	AAD49559.3		AAT_I	7,9-LDS
Podospora anserina	Ascomycota	CAP60153.1	XP_001912671.1	PODANS_1_4690 (PaCOX1)	10-HODE/1-octen-3ol
Aspergillus nidulans	Ascomycota	AAX35769.1			PpoB
Coccidioides immitis	Ascomycota	EAS28473.3	XP_001240056.2	CIMG_09677	8R-DOX-AOS
Zymoseptoria tritici	Ascomycota	EGP83657.1	XP_003848681.1	MYCGRDRAFT_49830	8S-DOX-AOS
Zymoseptoria tritici	Ascomycota	EGP87976.1	XP_003853000.1	MYCGRDRAFT_71165	9R-DOX-AOS
Aspergillus terreus	Ascomycota	AGH14485.1	XP_001211214.1	ATEG_02036	9(R),10-epoxy-10,12(Z)-octadecadienoic acid
Fusarium oxysporum	Ascomycota	EGU88194.1		FOXB_01332	9S-DOX-AOS
Glomerella graminicola	Ascomycota	EFQ27323.1	XP_008091343.1	GLRG_01818	9S-DOX-AOS
Fusarium oxysporum	Ascomycota	EGU79548.1		FOXB_09952	9R-DOX
Colletotrichum graminicola	Ascomycota	EFQ36675.1	XP_008100695.1	GLRG_11821	9R-DOX
Serpula lacrymans var. lacrymans	Basidiomycota	EGO22364.1	XP_007320902.1	SERLADRAFT_416857	unkown
Agaricus bisporus var. bisporus H97	Basidiomycota	EKV46570.1	XP_006461894.1	AGABI2DRAFT_143643	unkown
Coprinopsis cinerea	Basidiomycota	EAU90460.2	XP_001831297.2	CC1G_00844 (CcCOX1)	10(S)-HPODE
Fomitopsis pinicola	Basidiomycota	EPT00655.1		FOMPIDRAFT_99109	unkown
Rickenella mellea	Basidiomycota	TDL21822.1		BD410DRAFT_840230	unkown
Rickenella mellea	Basidiomycota	TDL21825.1		BD410DRAFT_279997	unkown
Schizophyllum commune	Basidiomycota	EFI97900.1	XP_003032803.1	SCHCODRAFT_11038	unkown
Fomitopsis pinicola	Basidiomycota	EPS97161.1		FOMPIDRAFT_83073	unkown
Agaricus bisporus var. bisporus H97	Basidiomycota	EKV43127.1	XP_006456120.1	AGABI2DRAFT_195360	unkown
Schizophyllum commune	Basidiomycota	EFI91160.1	XP_003026063.1	SCHCODRAFT_114799	unkown
Rickenella mellea	Basidiomycota	TDL18561.1		BD410DRAFT_842735	unkown
Coprinopsis cinerea	Basidiomycota	EAU86789.2	XP_001835023.2	CC1G_09914 (CcCOX2)	unkown
Pleurotus ostreatus PC15	Basidiomycota	KDQ24228.1		PLEOSDRAFT_1085502	unkown
Serpula lacrymans var. lacrymans	Basidiomycota	EGO25105.1	XP_007317227	SERLADRAFT_414828	unkown
Rickenella mellea	Basidiomycota	TDL26424.1		BD410DRAFT_520610	unkown
Fomitopsis pinicola	Basidiomycota	EPS97159.1		FOMPIDRAFT_95975	unkown
Fomitopsis pinicola	Basidiomycota	EPS97141.1		FOMPIDRAFT_1052690	unkown
Ustilago maydis	Basidiomycota	AAL38020.1			unkown
Serpula lacrymans var. lacrymans	Basidiomycota	EGO22766.1	XP_007320006.1	SERLADRAFT_439529	unkown
Rhizoctonia solani 123E	Basidiomycota	KEP52552.1		V565_043610	unkown
Rhizoctonia solani 123E	Basidiomycota	KEP54849.1		V565_012270	unkown
Rhizoctonia solani 123E	Basidiomycota	KEP46854.1		V565_178510	unkown

Table S2. Condition for multiple reaction monitoring to identify each hydroperoxide of fatty acid.

	Precursor ion* $[M+Na]^+$ (m/z)	Product ion* (m/z)	DP (V)	EP (V)	CE (V)	CXP (V)	Curtain gas (psi)	Ion source gas 1 (psi)	Ion source gas 2 (psi)	Collision Gas (psi)
16-HPOTrE	333.2	287.1	56	10	22	16.5	20	40.0	40.0	4.0
15-HPOTrE	333.2	246.1	59	10	18.8	13.5	20	40.0	40.0	4.0
13-HPOTrE	333.2	247.1	54	10	19.3	13.5	20	40.0	40.0	4.0
13-HPOTrE	333.2	206.1	58	10	17.6	11.5	20	40.0	40.0	4.0
10-HPOTrE	333.2	207.1	61	10	20.7	10.8	20	40.0	40.0	4.0
9-HPOTrE	333.2	195.1	59	10	14.3	9.8	20	40.0	40.0	4.0
13-HPODE	335.2	247.1	56	10	19.5	16	20	40.0	40.0	4.0
12-HPODE	335.2	206.1	75	10	17.5	10	20	40.0	40.0	4.0
10-HPODE	335.2	207.1	75	10	19	10	20	40.0	40.0	4.0
9-HPODE	335.2	195.1	55	10	13	10	20	40.0	40.0	4.0
10-HPOME	337.2	195.1	80	10	19.5	10	20	40.0	40.0	4.0
9-HPOME	337.2	207.1	80	10	23.6	10	20	40.0	40.0	4.0

HPOTrE; hydroperoxide of linolenic acid (octadecatrienoic acid), HPODE; hydroperoxide of linoleic acid (octadecadienoic acid), HPOME; hydroperoxide of oleic acid (octadecenoic acid)

Temperature: 600°C

Ion spray voltage: 5500 V

Source: Electrospray ionaization

Ion polarity: Positive

*LC-MS/MS analysis was carried out in the presence of sodium ion; thus, [M+Na]+ was detected as the molecular ion. The product ion diagnostic to the identication of the position of the hydroperoxy group was chosen (Ito et al., 2015).

Reference: Ito, J., Mizuochi, S., Nakagawa, K., Kato, S., and Miyazawa, T. (2015) Tandem mass spectrometry analysis of linoleic acid and arachidonic acid hydroperoxides via promotion of alkali metal adduct formation. *Anal. Chem.* 87, 4980-4987

Table S3. The domain structures of the proteins showing the highest homology to CcCOX1 within the respective class in the kingdom of fungi.

							Interpro superfamily	
Sub-division	Class	Genus	Species	NCBI acc.no.	ref	E-value with CcCOX1	Heam peroxidase sd	Cyt P450 sf
Basidiomycota	Pucciniomycotina	Leucosporidium	creatinivorum	ORY87519.1		0	+	+
	Ustilaginomycotina	Tilletia	indica	KAE8229188.1		0	+	+
	Agaricomycetes	Coprinopsis	cinerea	XP_001831297.2	this study	0	+	+
	Dacrymycetes	Dacryopinax	primogenitus	XP_040630007.1	PUBMED_22745431	0	+	+
	Tremellomycetes	Saitozyma	podzolica	RSH82924.1		5.00E-135	+	+
	Wallemiomycetes	Wallemia	hederase	TIA89457.1		1.00E-162	+	-
Ascomycota	Pezizomycetes	Morchella	conica	RPB15767.1	PUBMED_30420746	2.00E-163	+	+
	Orbilliomycetes	Arthrobotrys	flagrans	RVD83969.1	PUBMED_30917129	4.00E-173	+	+
	Eurotiomycetes	Aspergilllus	terreus	AFB71132.1		0	+	+
	Dothideomycetes	Westerdykella	ornata	XP_033652023.1	DOI: 10.1016/j.simyco.2020.01.003	0	+	+
	Lecanoromycetes	Gomphillus	americanus	CAF9919921.1		7.00E-166	+	+
	Leotiomycetes	Pseudogymnoascus	s. VKM F-4519	KFZ07385.1	PUBMED_25994131	0	+	+
	Sordariomycetes	Metarhizium	robertsii	XP_007816192.1	PUBMED 25368161	0	+	+
	Xylonomycetes	Xylona	heveae	XP_018185456.1	PUBMED_26693682	5.00E-177	+	+
	Saccharomycotina	Trichomonascus	ciferrii	KAA8901464.1	PUBMED_31575637	2.00E-168	+	+
	Taphrinomycotina	Saitoella	complicata	GAO49361.1	PUBMED_24646756	3.00E-72	+	-
Mucoromycota	Glomeromycotina	Rhizophagus	clarus	GBC07128	https://doi.org/10.1186/s12864-018-4853-0	6.00E-138	+	-
	Mortierellomycotina	Entomortierella	beljakovae	KAF9432922.1	PUBMED_33364917	3.00E-90	+	-
	Mucoromycotina	Umbelopsis	isabelina	KAG2183470.1	DOI: 10.3389/fmicb.2021.636986	2.00E-99	+	-
Zoopagomycota	Zoopagomycotina	na	na	no hit			-	-
	Entomophthoromycotina	Basidiobolus	meristosporus	ORX79743.1		6.00E-108	+	-
	Kickxellomycotina	na	na	no hit			-	-
Blastocladiomycota		na	na	no hit			-	-
Chytridiomycota	Chytridiomycetes	Rhizoclosmatium	globosum	ORY30110.1		2.00E-77	+	-
	Monoblepharidomycetes	na	na	no hit			-	-
	Neocallimastigomycetes	na	na	no hit			-	-
Microsporidia		na	na	no hit			-	-
Cryptomycota		na	na	no hit			-	-
Genes showing a significant homology in the organisms other than fungi.								
Magnoliophyta	Magnoliopsida	Carpinus	fangiana	KAB8343050.1		1.00E-167	+	+
		Qurcus	suber	XP_023877369.1		2.00E-161	+	+
Rotifera	Bdelloidea	Rotaria	magnacalcarata	CAF2064440.1		1.00E-113	+	-
		Adineta	steineri	CAF1363805.1		1.00E-113	+	-

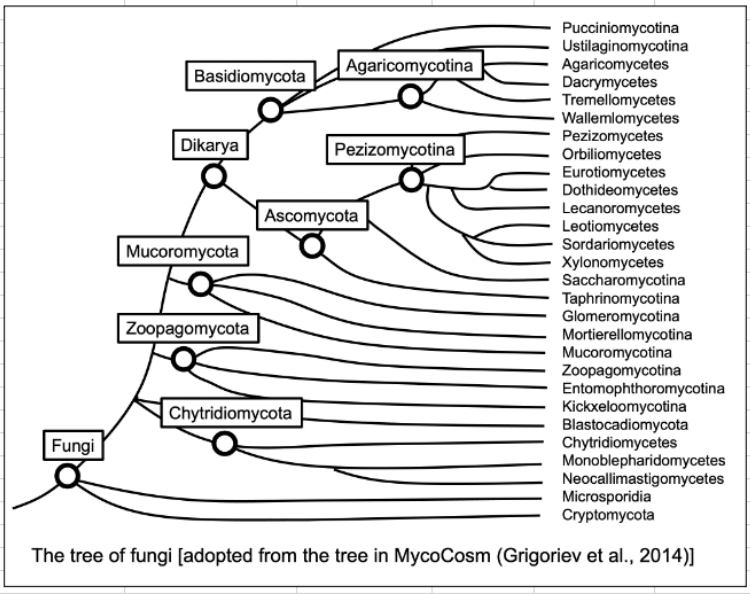

The tree of fungi [adopted from the tree in MycoCosm (Grigoriev et al., 2014)]

Table S4. Primers used in this study.

Primer	Sequence (5' --> 3')	Target gene	Gene ID	Usage
SV13	AAAGAAGCAGCCCTGGAGGAG	CcDOX1	CC1G_00844	Gene-disruption
SV14	TGACCTTCCATCTGACCCCAC	CcDOX1	CC1G_00844	Gene-disruption
SV17	ACGTCGTGACTGGGAGCTTGATGGGGTCAGTGGGG	CcDOX1	CC1G_00844	Gene-disruption
SV18	CCTGTGTGAAATTGTATCCAAGCCCTCGTGTGTCG	CcDOX1	CC1G_00844	Gene-disruption
SV21	AGCCCGCTCGTATATCGCAC	CcDOX1	CC1G_00844	Gene-disruption
SV22	ATCCGAACCGCTGAAAACCC	CcDOX1	CC1G_00844	Gene-disruption
SV24	TGGAAGCAACAAGAGACGGTC	CcDOX1	CC1G_00844	Gene-disruption
TN40	ACCCTTTCCCCCAAAATTTGGAAGC	pPHT1 (hph)		Gene-disruption
TN41	ACCTTCTGGCATGACCTTTTGATGATCGC	pPHT1 (hph)		Gene-disruption
TN1009	TGGCCTGAATGCACAATTACGG	CcDOX1	CC1G_00844	Gene-disruption
M13F	GTAAAACGACGGCCAGT	pBluescript II		Gene-disruption
M13R	CAGGAAACAGCTATGAC	pBluescript II		Gene-disruption
CcDOX1F	CCACCGGTCGCCACCATGTCGTCAAGCAAGGTCAAGC	CcDOX1	CC1G_00844	Expression of recombinant protein
CcDOX1(+EGFP)R	GCCCTTGCTCACCATGGCAGCATCGTACAATACGGAA	CcDOX1	CC1G_00844	Expression of recombinant protein
CcDOX1(-EGFP)R	ACTTTGGCGGCCGCTTTAGGCAGCATCGTACAATACG	CcDOX1	CC1G_00844	Expression of recombinant protein
CcDOX2F	CCACCGGTCGCCACCATGTCTTCCATCCTTCGCAAGC	CcDOX2	CC1G_09914	Expression of recombinant protein
CcDOX2(+EGFP)R	GCCCTTGCTCACCATCGCAACCTGGTACTGCAGAATC	CcDOX2	CC1G_09914	Expression of recombinant protein
CcDOX2(+EGFP)R	ACTTTGGCGGCCGCTTCACGCAACCTGGTACTGCAGA	CcDOX2	CC1G_09914	Expression of recombinant protein
pA3vector(+EGFP)F	ATGGTGAGCAAGGGCGAGGAGCTGT	pA3hr5		Expression of recombinant protein
pA3vector(-EGFP)F	AGCGGCCGCCAAAGTTGTTTCTGAC	pA3hr5		Expression of recombinant protein
pA3vectorR	GGTGGCGACCGGTGGATCCTTGAAT	pA3hr5		Expression of recombinant protein
qPCR-b-tubulin-For	GTA ACTCCACCGCCATCCAG	β-tubulin	CC1G_04743	RT-qPCR
qPCR-b-tubulin-Rev	GACCTCATCCTCGTATTCACC C	β-tubulin	CC1G_04743	RT-qPCR
qPCR-COXL1-For	CAACCAGAGCCGTGAAGAGTC	CcDOX1	CC1G_00844	RT-qPCR
qPCR-COXL1-Rev	ATTCAGGTCGGTTGTCGGTC	CcDOX1	CC1G_00844	RT-qPCR
qPCR-COXL2-For	GTCTGAACCCTGCCATTCCA	CcDOX2	CC1G_09914	RT-qPCR
qPCR-COXL2-Rev	CAAGACCGCTCCTTTCCCTTG	CcDOX2	CC1G_09914	RT-qPCR